Hindawi Publishing Corporation
Journal of Chemistry
Volume 2014, Article ID 784824, 8 pages
http://dx.doi.org/10.1155/2014/784824

Research Article

Galvanic Displacement of Gallium Arsenide Surface: A Simple and Low-Cost Method to Deposit Metal Nanoparticles and Films

Ngoc Duy Pham, Seok Ju Park, Jun Pil Lee, and Ilwhan Oh

Department of Applied Chemistry, Kumoh National Institute of Technology, Yangho-dong 1, Gumi-si, Gyeongbuk-do 730-701, Republic of Korea

Correspondence should be addressed to Ilwhan Oh; ioh@kumoh.ac.kr

Received 27 March 2014; Revised 3 July 2014; Accepted 17 July 2014; Published 13 August 2014

Academic Editor: Mallikarjuna N. Nadagouda

Herein, we report galvanic displacement of metal nanoparticles and films onto single-crystalline GaAs (100) substrates, a simple and cost-effective method to fabricate highly controlled metal/semiconductor interface. A time-resolved surface analysis of Au/GaAs system was conducted and microscopic mechanism of galvanic displacement was elucidated in detail. Quantitative temporal XPS measurements of the Au/GaAs interface showed that, initially, fast Au growth was slowed down as the deposition process proceeded. This was attributed to growing oxide layer blocking hole conduction and causing quenching of the deposition process. Addition of various inorganic acids, which function as oxide etchants, was found to enhance deposition rates by effectively removing surface oxide, with HF the most effective. Various precious metals, such as Pt and Ag, could be deposited onto GaAs through galvanic displacement, which demonstrates the versatility of the method.

1. Introduction

Metal nanoparticles and films on semiconductor are critical components in many devices. Representative examples are rectifying (Schottky) and ohmic junctions for integrated circuits [1]. Traditionally, vacuum deposition techniques, such as thermal evaporation and sputtering, have been used to deposit metals on semiconductor materials; these processes generally require expensive vacuum-based instruments [2–4]. Alternatively, solution-based methods, such as electrodeposition, are relatively inexpensive and can produce ultrathin metal nanoparticles and micrometer-thick films, depending on plating condition and bath composition [5]. This work focuses on *electroless* deposition, a method that does not require an external power source or electrical contacts, which are cumbersome in the metallization of semiconductor substrates.

Generally, an electroless deposition solution is composed of a metal salt to be deposited and a reducing agent to be oxidized on the surface of either metal deposits or the substrate and to reduce the metal ions during the process. In galvanic displacement (GD), a type of electroless deposition, the semiconductor substrate itself functions as the reducing agent, providing electrons to reduce metal ions [6–8]. (Figure 1) Ideally, the oxidized substrate layer should be effectively dissolved and a pristine nonoxidized surface should be regenerated for the GD process to continue. The rate and extent of this process can be controlled by deposition time, metal ion concentration, and presence of oxide etchants that remove oxide from the surface. Metal-semiconductor structures fabricated via GD, usually in the form of uniformly distributed metal nanoparticles on semiconductor surfaces, have found use in various applications. For example, in metal-assisted chemical (MAC) etching, electroless metal deposition onto Si substrate is most widely used to deposit catalyst layer, which functions as catalyst to provide holes to local region [9]. Another example is the deposition of a catalyst on photoelectrodes for solar water splitting [10].

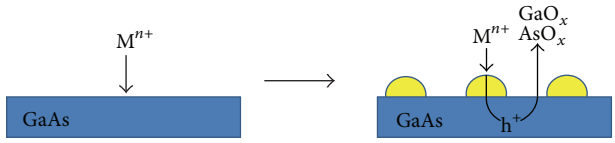

Figure 1: Mechanism of galvanic displacement of GaAs substrate with metal.

Because neither hydrogen nor oxygen evolution on bare semiconductor surfaces is fast enough, a catalyst is usually deposited on photoelectrode surfaces to facilitate the water splitting reaction. Electroless deposition of precious metals (i.e., Pt) is a convenient and effective method to deposit metal catalysts onto photoelectrodes. Recent reports show that, in the case of Pt/p-Si photoelectrodes, electroless deposition of catalyst materials is necessary for the photoelectrode to work properly [11]. Evaporated Pt/Si showed negligible photovoltage. Furthermore, electroless deposition has been utilized to deposit metal nanoparticles onto vertically aligned high-aspect ratio semiconductor structures [12–14]. Vacuum deposition of metals onto these structures is commonly difficult due to the unidirectional flux of metal atoms in vacuum deposition.

Gallium arsenide (GaAs) is the second most widely studied semiconductor material, only next to silicon [15]. Unlike Si, which has indirect low band gap (1.1 eV), GaAs has a direct band gap of 1.4 eV, which leads to strong absorption and optimal conversion of solar irradiation. Furthermore, the carrier mobility of GaAs is much higher than that of Si, making GaAs suitable for high-speed applications. Electroless metal deposition onto Si materials has been studied extensively, but studies with GaAs materials are relatively rare. Motivated by technological importance of the III–V/metal interface, electroless Au deposition onto patterned GaAs surface was investigated [16, 17]. Furthermore, a detailed analysis of metal/GaAs interface confirmed existence of sandwiched intermetallic layer at the interface [18].

In this work, we have conducted time-resolved measurements of GaAs galvanic displacement with precious metals (Au, Pt, Ag). Our detailed temporal analysis of interface sheds more light on mechanism of the GD process. Quantitative surface measurement shows that, initially, fast metal growth rate is slowed down, as GD process proceeds. Time-resolved XPS measurements directly confirm growing oxide in underlying GaAs substrate, which probably quenches GD process by blocking hole conduction. Addition of inorganic acids, which function as oxide etchants, was found to enhance deposition rates by effectively removing surface oxide. Overall, this paper reports on the electroless metal deposition on the widely used GaAs materials in the technologically important thickness range. Ultimately, enabling and understanding electroless deposition of metals onto technologically relevant GaAs will lead to versatile utility in microelectronic metallization, catalyst for energy conversion, and so forth.

2. Experimental

2.1. GaAs Substrates and Pretreatment. A single-side polished n-type GaAs (100) wafer (Neo Semitech; Si-doped semiconducting) was used as the substrate for the electroless deposition experiments. The GaAs wafer was first degreased, by rinsing with acetone, isopropyl alcohol, and ultrapure deionized water (DIW) in sequence, then it was cleaved into ~1 cm × 1 cm pieces. To remove native surface oxides, the GaAs samples were immersed in dilute HCl (1 : 10 v/v) for 5 min. After removal of native oxide, care is taken to minimize the exposure time to air.

2.2. Metal Deposition. The pristine GaAs surface was immersed in metal salt solutions of various concentrations. $HAuCl_4 \cdot 4H_2O$ was purchased from the Wako Company and H_2PtCl_6 (98%) was obtained from Sigma-Aldrich. $AgNO_3$ (99.8%), HCl (ultrapure grade), and H_2SO_4 (ultrapure grade) were purchased from Daejung Chemical. HF (ACS grade) was purchased from JT Baker. After metal deposition, GaAs sample was taken out of deposition bath and was thoroughly rinsed with ultrapure water then dried under N_2 stream.

2.3. Characterization. The metal nanostructures fabricated by galvanic displacement were characterized by scanning electron microscopy (SEM) and X-ray photoelectron spectroscopy (XPS). SEM measurements were carried out using a JEOL/JSM-6701F instrument. Particle size analysis was performed using ImageJ software (NIH). XPS measurements were carried out using a ThermoFisher K-Alpha spectrophotometer with a monochromatic Al Kα source. NIST IMFD database was utilized to find inelastic mean free path of electrons in solids [19].

3. Results and Discussion

The previously proposed mechanism for galvanic displacement (GD) metal deposition on GaAs is shown in Figure 1. Initially, a metal ion is reduced on the semiconductor surface and produces holes (h^+) into the semiconductor in the following reaction:

$$M^{n+} \longrightarrow M\,(s) + n \cdot h^+, \tag{1}$$

where M^{n+} represents a metal ion in oxidation state n. To start, reaction (1) occurs on the bare surface, and metal seeds are nucleated on the GaAs surface. As the GD process proceeds, more and more metal atoms deposit preferentially on the metal seeds and grow in size. The holes generated in the reaction transfer to the semiconductor/electrolyte interface, where GaAs is oxidized and dissolved into the electrolyte according to reaction (2):

$$GaAs + (3 + n)\,h^+ \longrightarrow Ga^{3+} + As^{n+}, \tag{2}$$

where n is either 3 or 5. In the case of GD on Si, a stable, robust oxide forms on the surface, and an additional etching agent (i.e., HF) is necessary to effectively remove the oxide. Otherwise, the GD process will halt because the surface oxide

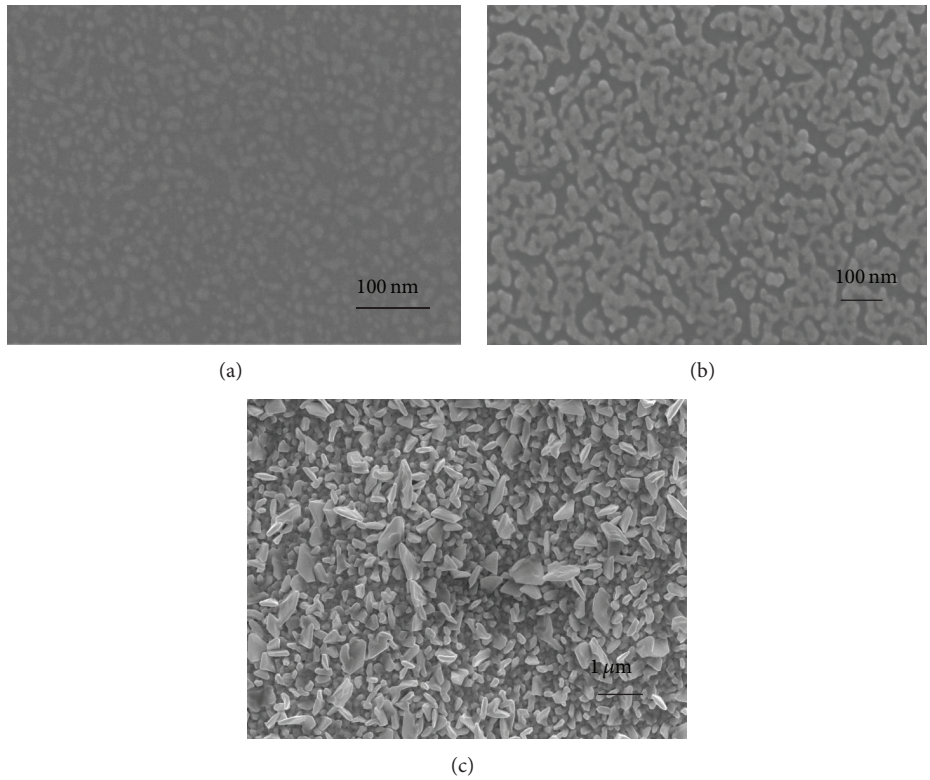

FIGURE 2: SEM images of GaAs (100) substrates immersed in dilute $HAuCl_4$ solution. $HAuCl_4$ concentration and deposition duration were (a) 0.7 mM; 20 s, (b) 1.0 mM; 30 s, and (c) 1.0 mM; 60 min.

blocks the further oxidation of Si. On the other hand, for GaAs, which is known to form less stable, soluble surface oxides, oxidation of GaAs results partly in dissolution of GaAs materials and partly in surface oxide formation, as will be shown in the following results.

Figure 2 shows SEM micrographs of the electroless GD deposition of Au onto single-crystalline GaAs (100) substrate. Freshly prepared GaAs (100) surface was immersed in dilute $HAuCl_4$ solution for designated duration of time. As Figure 2(a) shows, the initially bare GaAs surface is covered with nanoparticles a few seconds after immersion in the deposition bath. The average size of the nanoparticles is 16 ± 2 nm after 20 s of immersion in 0.7 mM $HAuCl_4$. In Figure 2(a), the SEM image contrast of metal nanoparticles to underlying substrate is low, indicating a short nanoparticle height. But the contrast becomes higher as the nanoparticles grow in size. The nanoparticles grow rapidly and coalesce with each other, forming networks of nanoparticles as shown in Figure 2(b). After extensive Au plating, the GaAs substrate is covered with a thick film of Au crystallites, as shown in Figure 2(c), and the underlying GaAs substrate is no longer visible at this stage.

For qualitative and quantitative analysis of electroless Au deposits on GaAs substrate, X-ray photoelectron spectroscopy (XPS) was performed on the Au/GaAs samples. The presence of Au peak in Figure 3 doubtlessly confirms that the observed nanoparticles are Au deposits. As expected, the Au $4f_{7/2}$ peak increases as the deposition time is increased.

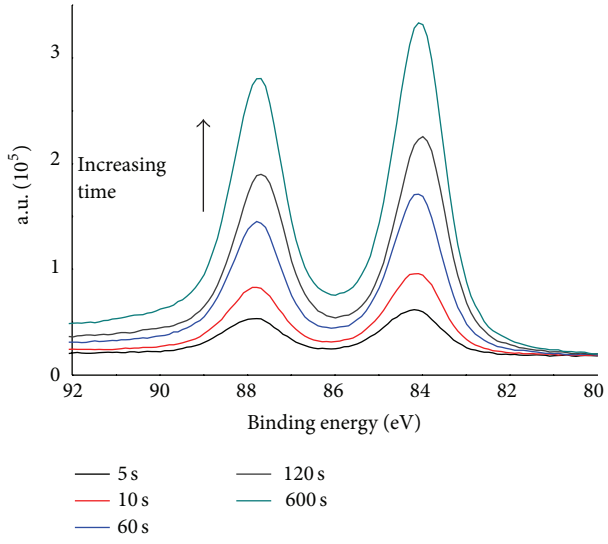

FIGURE 3: XPS spectra in the Au $4f_{7/2}$ region for GaAs (100) samples immersed in 0.1 mM $HAuCl_4$ for increasing duration.

Neither a shift nor a satellite peak in the Au $4f_{7/2}$ peak is observed, indicating that the deposit is metallic Au with little oxidized Au ions from the deposition bath. On the other hand, Figure 4(a) shows the Ga 3d peak from the underlying substrate. The Ga 3d peak is composed of two peaks, one at

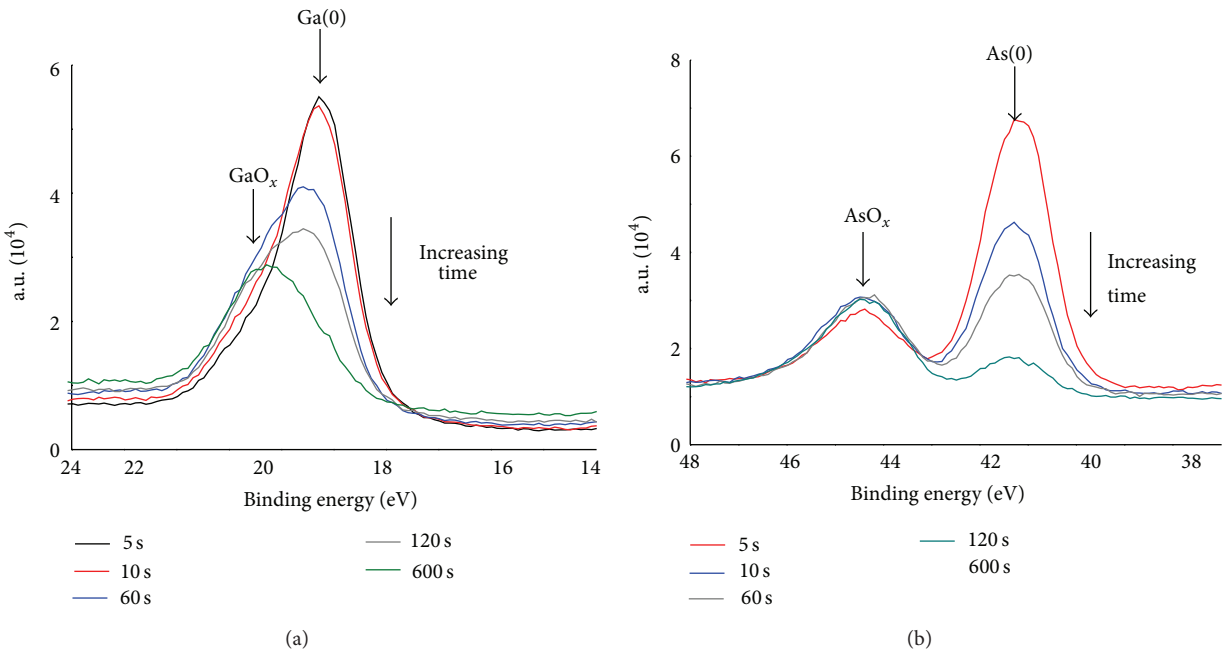

Figure 4: XPS spectra (a) in the Ga 3d region and (b) in the As 3d region for GaAs (100) samples immersed in 0.1 mM $HAuCl_4$ for increasing duration.

19.3 eV for Ga(0) and the other at 20.3 eV for GaO_x. Initially, the Ga(0) peak is much stronger than the GaO_x peak. As GD proceeds and the substrate becomes covered with Au, the Ga(0) peak diminishes and ultimately disappears. This is because the growing Au thin film increasingly blocks more photoelectrons from the GaAs substrate (the mean free path of electrons in Au is 1.78 nm [19]). The overall results indicate that, as the GD process proceeds, Ga is oxidized and a significant amount of GaO_x is formed on the surface. The As 3d peaks in Figure 4(b) show the temporal evolution that is consistent with the aforementioned Ga 3d peaks. The initially strong peak from As(0) located at 41.2 eV diminishes as Au covers the substrate. However, the weak peak for AsO_x at 44.4 eV increases as AsO_x is formed on the surface.

As the intensities of the Au and Ga peaks are directly affected by the deposition of Au, the thickness of Au film can be determined from the ratio of I_{Au} and I_{Ga} via (3) [20]:

$$d = \lambda_{Au} \ln\left(1 + \frac{I_{Au}/S_{Au}}{I_{Ga}/S_{Ga}}\right), \quad (3)$$

where λ_{Au} is the mean free path of electrons in Au, I_i the XPS intensity of element i, and S_i the sensitivity factor of element i. Figure 5 shows the evolution of Au thickness as deposition progresses in different concentration of Au salt. Naturally, deposition in concentrated solutions is faster than for dilute solutions. From the measurement, the electroless deposition can be divided into two domains. In the first domain, at the initial stage of electroless deposition, the growth rate is quite high. In this domain, surface coverage of Au is relatively low and the bare GaAs surface is available for oxidation, resulting in a high deposition rate. In the second time domain, the underlying GaAs substrate is nearly fully covered by an oxide layer and a relatively thick Au film, which hinders the further substrate oxidation and mass transfer. This results in a relatively low deposition rate.

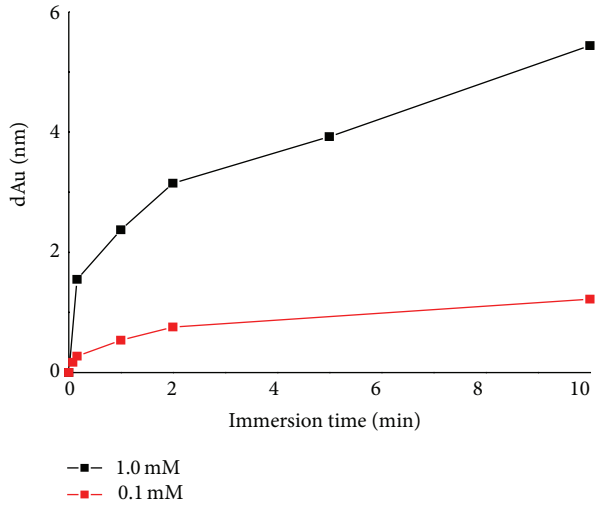

Figure 5: Growth of Au thin films when GaAs (100) sample is immersed in two different concentrations of $HAuCl_4$.

Figure 6 shows cross-sectional SEM images of the Au/GaAs, which verify the intimate interface between the Au deposits and the GaAs substrate. Note that the Au deposit is not a uniform film but is composed of an array of nanoparticles. With reference to the film thickness determined by the XPS measurements, the height of the individual Au nanoparticles is relatively larger; for example, for the Au/GaAs deposited for the duration of 2 min, the average

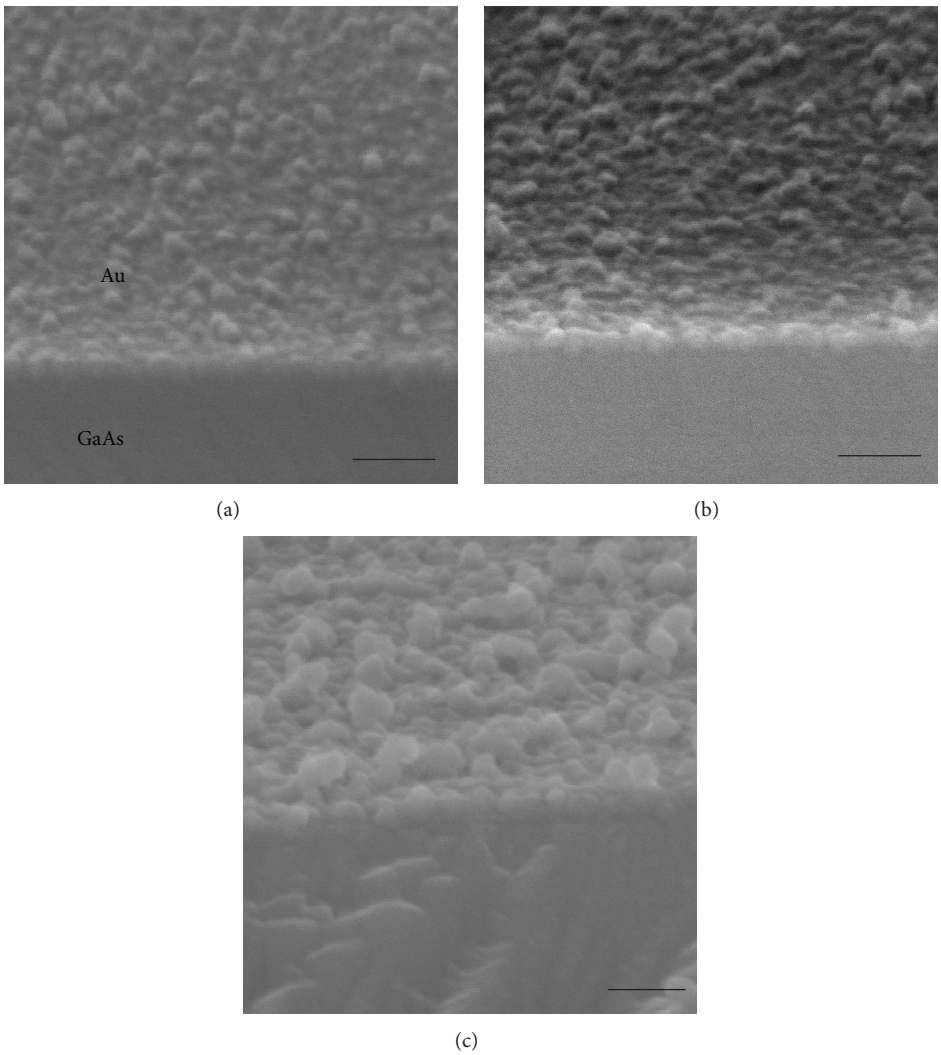

Figure 6: Cross-sectional scanning electron microscope (SEM) image of galvanic displacement process on the GaAs (100) substrate. Cleaned GaAs (100) sample is immersed in 0.5 mM $HAuCl_4$ for (a) 1 min, (b) 2 min, and (c) 10 min. Scale bars are 90 nm.

height of the Au nanoparticles was ~25 nm, whereas the XPS measurements give ~2 nm film thickness. The difference indicates that the Au deposit contains significant portion of voids, as is evident in Figure 2. The film thickness determined by the XPS measurements in Figure 5 can be interpreted as average value over the Au nanoparticles and voids.

As verified by XPS measurements, the initial, high GD rate is retarded by the growing surface oxide. For this reason, galvanic displacement of metal onto a semiconductor surface usually requires an etching agent that effectively removes the surface oxide. For example, galvanic displacement onto Si is almost always conducted in HF-based solutions; HF dissolves surface SiO_2 that will otherwise block further GD. It is well known that several inorganic acids, including HCl, H_2SO_4, and HF, can etch GaAs oxides [15]. Figure 7 shows the effect of various inorganic acids on the galvanic displacement of Au/GaAs. Whereas the addition of HCl has little effect on the thickness of the thin film, deposition rates with H_2SO_4 and HF increase significantly; of the two inorganic acids, HF

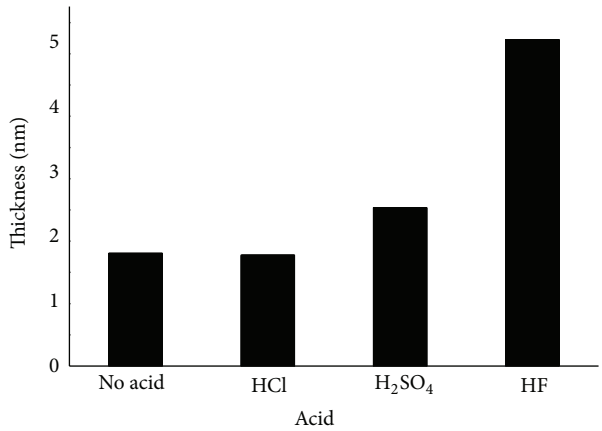

Figure 7: Effect of inorganic acids on thickness of Au thin films. Galvanic displacement is conducted in 1.0 mM, $HAuCl_4$ solution containing plating bath which includes 0.8 M HCl, 4.6 M H_2SO_4, or 3.3 M HF for 3 min.

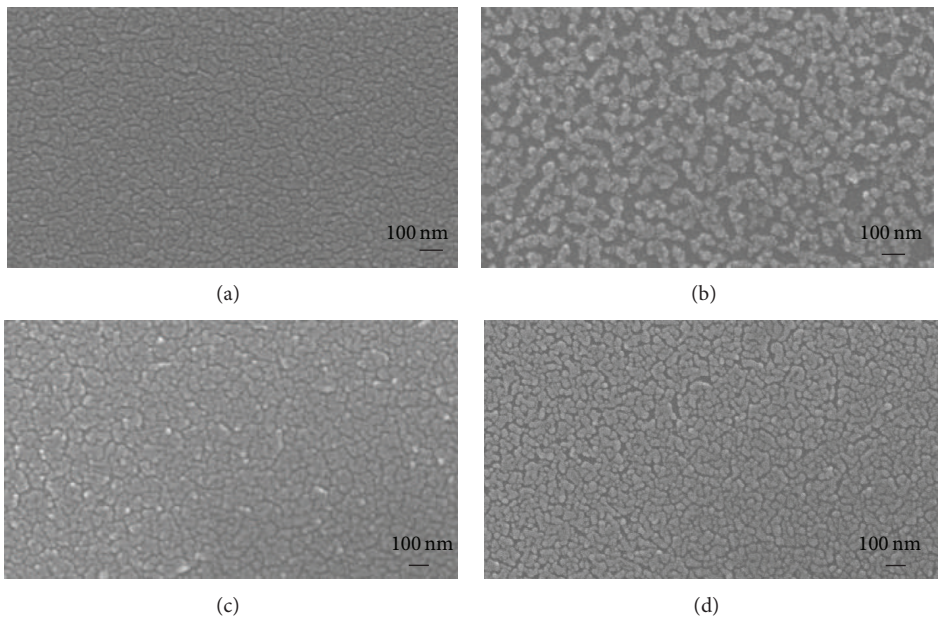

Figure 8: SEM images of Au thin films deposited in the presence of inorganic acids. Galvanic displacement is conducted for 3 min in 1.0 mM $HAuCl_4$ solution containing (a) no acid, (b) 0.8 M HCl, (c) 4.6 M H_2SO_4, and (d) 3.3 M HF.

is known to effectively remove surface GaAs oxides [15]. As experimentally verified by XPS measurements, the growth of surface oxides during the GD process retards the GD process by blocking the hole from the deposited metal ion. Thus, effective etching of the surface oxides by inorganic acids enhances the GD rate. Figure 8 compares morphologies of the Au thin films deposited by the GD process in the presence of various inorganic acids. Au films deposited with no acid and HCl exhibit cracks and uncovered areas through which the underlying GaAs substrate is visible; it is likely that the surface oxide forms on the exposed substrate where no Au is deposited. On the other hand, the Au films deposited with H_2SO_4 and HF look closely packed and dense, with no underlying substrate visible. The inorganic acids function as oxide etchants, effectively removing the surface oxides, resulting in different surface morphologies.

Although this paper focuses mainly on the GD of Au onto GaAs substrates, a number of other metals can be deposited via GD. The valence band edge (E_{VB}) of GaAs is positioned at ca. +0.3 V versus SHE. (Figure 9). Spontaneous deposition occurs when the standard potential (E°) of metal ions is larger (downward direction in Figure 9) than E_{VB}, such that the holes from the metal are injected into the GaAs valence band. The E° value for $AuCl_4^-/Au(0)$ is 0.93 V and the potential difference ($E^\circ - E_{VB}$) provides a large driving force for Au deposition. Pt and Ag also have large E° values, such that they can be spontaneously deposited onto GaAs via GD process. SEM images of Pt and Ag nanoparticles deposited onto GaAs substrates via GD are shown in Figure 10. Compared to Au deposition on GaAs, deposition rates for these metals are slower and surface coverage is lower, likely due to the lower E° values for Pt and Ag. Additionally, the Ag nanoparticles exhibit a more faceted morphology. This phenomenon was also observed for Au/InP (100) substrates [16].

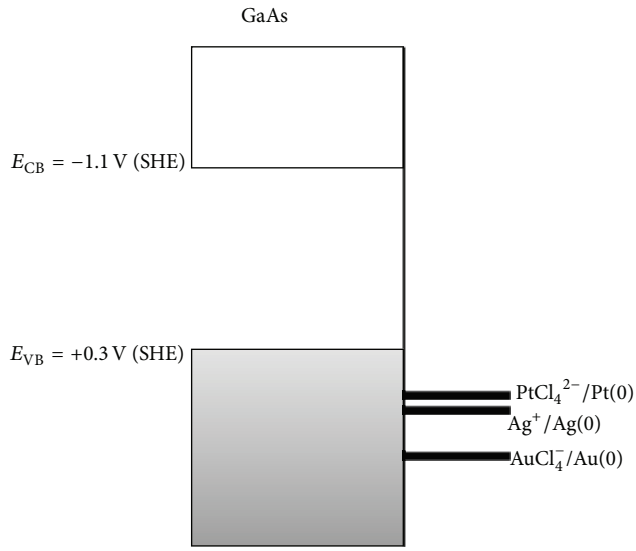

Figure 9: Schematic diagram of interfacial energetics of GaAs and relevant metal ions.

4. Conclusion

Electroless deposition of metals onto GaAs was investigated in order to elucidate the mechanism and experimental factors that affect deposition rates and morphology. When GaAs (100) substrates were immersed in dilute Au salt solutions,

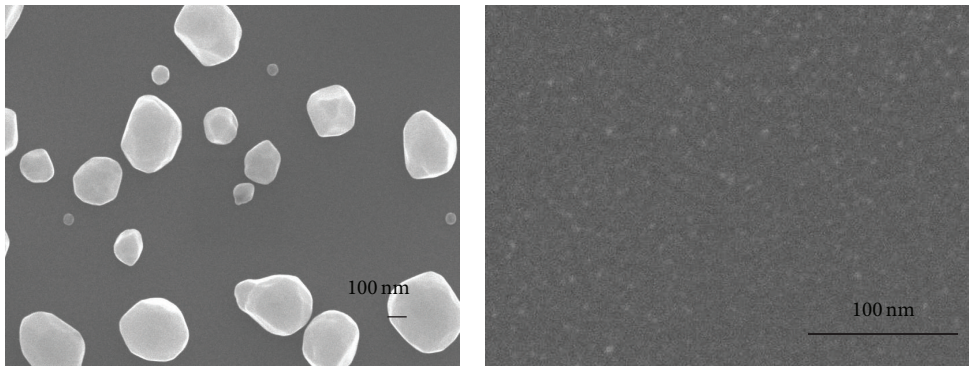

(a) (b)

Figure 10: Galvanic displacement of GaAs with various metals, (a) Ag and (b) Pt.

Au nanoparticles were initially deposited; the nanoparticles subsequently grew in size and ultimately formed thin films. This behavior is in contrast to the galvanic displacement of metals on Si surfaces, where, in the absence of HF, metal deposition ceases when the Si surface becomes covered with oxides. Even in our Au/GaAs system, XPS measurement confirmed existence of surface oxides generated from the GD process. However, these oxides are not robust enough to completely limit the GD process.

Quantitative XPS measurements of the Au/GaAs interface showed that Au growth was initially fast but was slowed down as the GD process proceeded. At the same time, temporal XPS analysis revealed that an oxide layer grew in the underlying GaAs substrate. We speculate that growing oxide layer blocks hole conduction and causes quenching of the GD process. In addition, growing top-most Au layer is likely to hinder mass transfer of oxidation products, contributing to the reduced deposition rate. Addition of inorganic acids, which function as oxide etchants, was found to enhance deposition rates by effectively removing surface oxide. Also, other than Au, various precious metals, such as Pt and Ag, were deposited onto GaAs via the GD process onto GaAs, which demonstrates the versatility of the GD method.

Conflict of Interests

The authors declare that there is no conflict of interests regarding the publication of this paper.

Acknowledgment

This paper was supported by Research Fund, Kumoh National Institute of Technology.

References

[1] S. M. Sze, *Semiconductor Devices: Physics and Technology*, John Wiley & Sons, New York, NY, USA, 2002.

[2] S. A. Campbell, *The Science and Engineering of Microelectronic Fabrication*, Oxford University Press, 2004.

[3] M. Madou, *Fundamentals of Microfabrication*, CRC Press LLC, New York, NY, USA, 1997.

[4] K.-N. Tu, J. W. Mayer, and L. C. Feldman, *Electronic Thin Film Science for Electric Engineers and Materials Scientists*, Macmillan, 1992.

[5] G. Oskam, J. G. Long, A. Natarajan, and P. C. Searson, "Electrochemical deposition of metals onto silicon," *Journal of Physics D: Applied Physics*, vol. 31, no. 16, pp. 1927–1949, 1998.

[6] M. Aizawa, A. M. Cooper, M. Malac, and J. M. Buriak, "Silver nano-lnukshuks on germanium," *Nano Letters*, vol. 5, no. 5, pp. 815–819, 2005.

[7] L. A. Porter Jr., H. C. Choi, J. M. Schmeltzer, A. E. Ribbe, L. C. C. Elliott, and J. M. Buriak, "Electroless nanoparticle film deposition compatible with photolithography, microcontact printing, and dip-pen nanolithography patterning technologies," *Nano Letters*, vol. 2, no. 12, pp. 1369–1372, 2002.

[8] L. A. Porter Jr., H. C. Choi, A. E. Ribbe, and J. M. Buriak, "Controlled electroless deposition of noble metal nanoparticle films on germanium surfaces," *Nano Letters*, vol. 2, no. 10, pp. 1067–1071, 2002.

[9] Z. Huang, N. Geyer, P. Werner, J. de Boor, and U. Gösele, "Metal-assisted chemical etching of silicon: a review," *Advanced Materials*, vol. 23, no. 2, pp. 285–308, 2011.

[10] M. G. Walter, E. L. Warren, J. R. McKone et al., "Solar water splitting cells," *Chemical Reviews*, vol. 110, no. 11, pp. 6446–6473, 2010.

[11] J. R. McKone, E. L. Warren, M. J. Bierman et al., "Evaluation of Pt, Ni, and Ni-Mo electrocatalysts for hydrogen evolution on crystalline Si electrodes," *Energy and Environmental Science*, vol. 4, no. 9, pp. 3573–3583, 2011.

[12] I. Oh, J. Kye, and S. Hwang, "Enhanced photoelectrochemical hydrogen production from silicon nanowire array photocathode," *Nano Letters*, vol. 12, no. 1, pp. 298–302, 2012.

[13] S. W. Boettcher, E. L. Warren, M. C. Putnam et al., "Photoelectrochemical hydrogen evolution using Si microwire arrays," *Journal of the American Chemical Society*, vol. 133, no. 5, pp. 1216–1219, 2011.

[14] K. Peng, X. Wang, X. Wu, and S. Lee, "Platinum nanoparticle decorated silicon nanowires for efficient solar energy conversion," *Nano Letters*, vol. 9, no. 11, pp. 3704–3709, 2009.

[15] R. E. Williams, *Gallium Arsenide Processing Technology*, Artech House, 1984.

[16] M. R. Hormozi Nezhad, M. Aizawa, L. A. Porter Jr., A. E. Ribbe, and J. M. Buriak, "Synthesis and patterning of gold nanostructures on InP and GaAs via galvanic displacement," *Small*, vol. 1, no. 11, pp. 1076–1081, 2005.

[17] H. Lim, J. Noh, D. Choi, W. Kim, and R. Maboudian, "A simple soft lithographic nanopatterning of gold on gallium arsenide via galvanic displacement," *Journal of Nanoscience and Nanotechnology*, vol. 10, no. 8, pp. 5020–5026, 2010.

[18] S. Y. Sayed, B. Daly, and J. M. Buriak, "Characterization of the interface of gold and silver nanostructures on InP and GaAs synthesized via galvanic displacement," *The Journal of Physical Chemistry C*, vol. 112, no. 32, pp. 12291–12298, 2008.

[19] C. J. Powel and A. Jablonski, *NIST Electron Inelastic-Mean-Free-Path Database, Version 1.2, SRD 71*, National Institute of Standards and Technology, Gaithersburg, Md, USA, 2010.

[20] P. J. Cumpson, "The Thickogram: a method for easy film thickness measurement in XPS," *Surface and Interface Analysis*, vol. 29, pp. 403–406, 2000.